applied sciences

MDPI

Article

Passive Power Line Communication Filter Design and Benchmarking Using Scattering Parameters

Sebastian Avram * and Radu Vasiu

Faculty of Electronics, Telecommunications and Information Technologies, Politehnica University of Timisoara, Bd. Vasile Parvan, nr. 2, 300223 Timisoara, Romania; radu.vasiu@upt.ro
* Correspondence: sebastian.avram@student.upt.ro

Abstract: NB-PLC (narrowband power line communication) is a method of data communication that involves superimposing a relatively high-frequency signal (9 kHz to 500 kHz), which contains data, onto the power grid's low frequency (50 to 60 Hz) signal. While using the existing power grid as a transmission medium is convenient, the power grid was not designed for this purpose, leading to challenges such as conduction emission and infrastructure limitations. To overcome these technical challenges, passive filters are necessary. This article presents the design, simulation (using scattering parameters), and evaluation of an NB-PLC filter by comparing it to commercially available filters. Our proposed design and benchmarking methods enable the accurate prediction of the filter's behavior in field conditions. After comparing our filter with commercially available filters, we observed that it exhibits superior characteristics. Specifically, our filter has the best insertion loss versus frequency, achieved three times higher attenuation at 50 kHz (−130 dB) compared to the best commercially available filter (−40 dB), and has a power consumption of 0.6 W, which is comparable to the most power-efficient commercial filter (0.5 W). Additionally, our filter has the second best input and output impedance of 3.6 Ω within the frequency range of 35 kHz–95 kHz.

Keywords: power line communication (PLC); power grid; NB-PLC; smart grid; filters; conducted disturbances

Citation: Avram, S.; Vasiu, R. Passive Power Line Communication Filter Design and Benchmarking Using Scattering Parameters. *Appl. Sci.* **2023**, *13*, 6821. https://doi.org/10.3390/app13116821

Academic Editor: Pierluigi Siano

Received: 30 April 2023
Revised: 25 May 2023
Accepted: 1 June 2023
Published: 4 June 2023

Copyright: © 2023 by the authors. Licensee MDPI, Basel, Switzerland. This article is an open access article distributed under the terms and conditions of the Creative Commons Attribution (CC BY) license (https://creativecommons.org/licenses/by/4.0/).

1. Introduction

As of 2020, it is estimated that 43% of electricity consumers in the EU-28 (European Union) have SMs (smart meters) installed, amounting to 123 million [1]. It is expected that by 2024, the number of installed SMs will increase to 223 million and that by 2030 it will reach 266 million. A total of 16 countries out of EU-28 have chosen NB-PLC (Narrow band power line communication) as a communication method between SM and DC (data concentrator) [2]. The study performed by the Joint Research Centre [2] estimated higher rollout rates compared to [1], while a market study performed at the end of 2020 showed that 130 million smart meters had been rolled out in Europe out of which 72% use PLC [3].

In Europe, NB-PLC uses Cenelec A, B, C, and D bands (3 kHz up to 148.5 kHz) which is impacted by gaps in the electromagnetic compatibility (EMC) conducted emissions standardization and electromagnetic interferences (EMI). These two topics are the subjects of research articles [4–15] and have the attention of The Comité International Spécial des Perturbations Radioélectriques (CISPR) as well as the international electrotechnical commission (IEC). Efforts are underway to address this gap, including proposed changes to standards such as CISPR 16-1-2, CISPR 32, and subsequent IEC standards.

We have identified that only in the following cases do standards specify the emission limits in the 3–148.5 kHz frequency band: NB-PLC specific standard [16], lightning equipment [17], and one home appliance type (inductive ovens) from the home appliances EMC

standard [18]. Figure 1 graphically represents the IEC EMC standards that cover most equipment connected to the power grid in Europe and the frequency range they cover; for most of the standards there is no emission limit below 150 kHz.

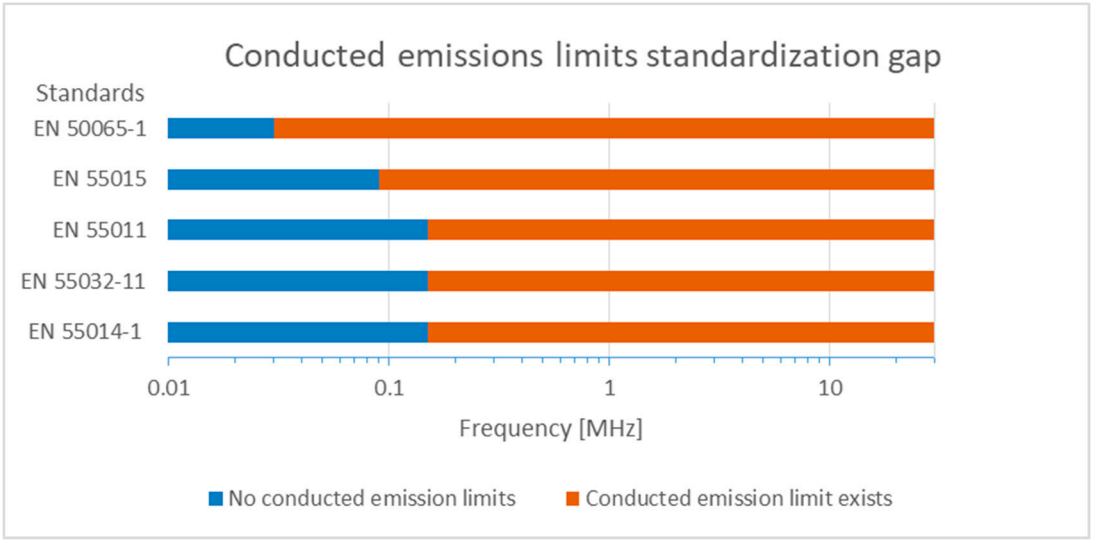

Figure 1. Summary of the most used EMC standards.

Mains connected switched-mode power supplies and inverters commonly utilize switching frequencies below 150 kHz, resulting in the generation of conducted emissions that impact NB-PLC [15,19]. The selection of switching frequencies below 150 kHz is motivated by several key factors [20]:

- Efficiency: lower switching frequencies can improve the overall efficiency of the SMPS. At lower frequencies, the switching losses in the power semiconductors, such as transistors or diodes, are reduced. This results in lower power dissipation and higher conversion efficiency;
- Electromagnetic interference (EMI): higher switching frequencies can generate more emissions due to increased harmonics and faster switching transitions. Relaxed or an absence of limits below 150 kHz contribute to this choice as well;
- Thermal management: switching components in SMPS can generate heat and operating at lower frequencies can help manage thermal issues. With reduced switching frequency, the components have more time to dissipate heat between each switching cycle;
- Component selection: some components used in SMPS, such as inductors and transformers, may have limitations at higher frequencies, including increased losses and size constraints.

The growing adoption of NB-PLC within smart grid applications, combined with existing standardization gaps and the presence of grid-connected devices that operate at switching frequencies below 150 kHz, necessitates the development of power line filters capable of providing significant attenuation within the Cenelec bands A, B, C, and D.

Passive filters were used for a long time [21–24] as a means of addressing conducted emissions in the power grid or to isolate different sections of a PLC network [25]. This article aims to contribute to this field of expertise by addressing several novel aspects. Firstly, it serves as a comprehensive source of information for designing and testing narrowband NB-PLC filters. Through an extensive literature review, it provides a complete understanding of the development, integration, and testing considerations associated with NB-PLC filters.

In addition, this research introduces a new approach by employing S-parameters (scattering parameters) for the design and simulation of NB-PLC filters. While the use of

S-parameters in design and simulation methods is not unprecedented [26,27], this study represents the first instance of applying this specific approach to NB-PLC filter design.

To demonstrate the efficacy of the proposed design methods described in this article, a 13th order power line filter was developed utilizing custom-made inductors. The designed filter exhibits high insertion loss characteristics below 150 kHz. It achieves a remarkable attenuation of −130 dB at 50 kHz while maintaining a low power consumption of 0.6 W with an input and output impedance of 3.6 Ω.

Through these findings, the article highlights the potential and advantages of employing the described methods for designing NB-PLC filters and offering improved performance in terms of insertion loss, attenuation, power consumption, and impedance characteristics.

The rest of the article is structured as follows:

Section 2 provides a comprehensive overview of the integration of power line filters into the power grid, highlighting the key services present in the grid and the two main types of power line filter topologies.

Section 3 presents the performance tests that ought to be conducted as an integral part of power line filter benchmarking. The relationship between testing methods and the actual conditions found in the power grid is also presented. By doing so, we aim to provide a better understanding of the factors that affect filter performance in real-world settings.

Section 4, in addition to Section 3, outlines the safety and immunity tests that should be conducted as part of benchmarking as well as the passive filter standard [28].

Section 5 presents the design, simulation, and evaluation of the proposed passive power line filter as well as a comparison with three commercially available filters. Our approach is pragmatic and uses S-parameters to facilitate the filter design process.

Section 6 presents the conclusions of our research activities presented in the article and proposes future work in this field of expertise.

2. Filters' Integration, Topologies, and Impact in the Power Grid

This section presents the basic types of PLC filters and their main characteristics as well as interferences between filters and other services in the power grid.

2.1. Integration of Power Line Filters in the Grid

Typically, power line communication filters are used in the smart grid in the following cases:

- Between the SM and the fuse box for filtering the conducted noise that is generated by the devices in the house [29]. If the filter does not require a ground connection or if the main fuse is not differential, it can be installed after the main fuse without any issues. However, if the filter does require a ground connection or if the main fuse is differential, installing the filter after the main fuse may cause the fuse to trip. This filter use case is labeled as Filter Type 1 in Figure 2;
- Between two sections of the power-line for separating NB-PLC devices from two areas which are connected to the same voltage transformer. The division in two areas ensures that the SM using NB-PLC from each area connects to the PLC-DC (power line communication data concentrator) they are supposed to. This type of filter installation is required when there are many SM connected to a branch and an additional DC is installed so that the data-rate is improved [25]. This filter use case is labeled as Filter Type 2 in Figure 2.

Figure 2 represents the two general use cases of PLC filters in the low voltage smart grid. For simplicity reasons, only single-phase devices are shown.

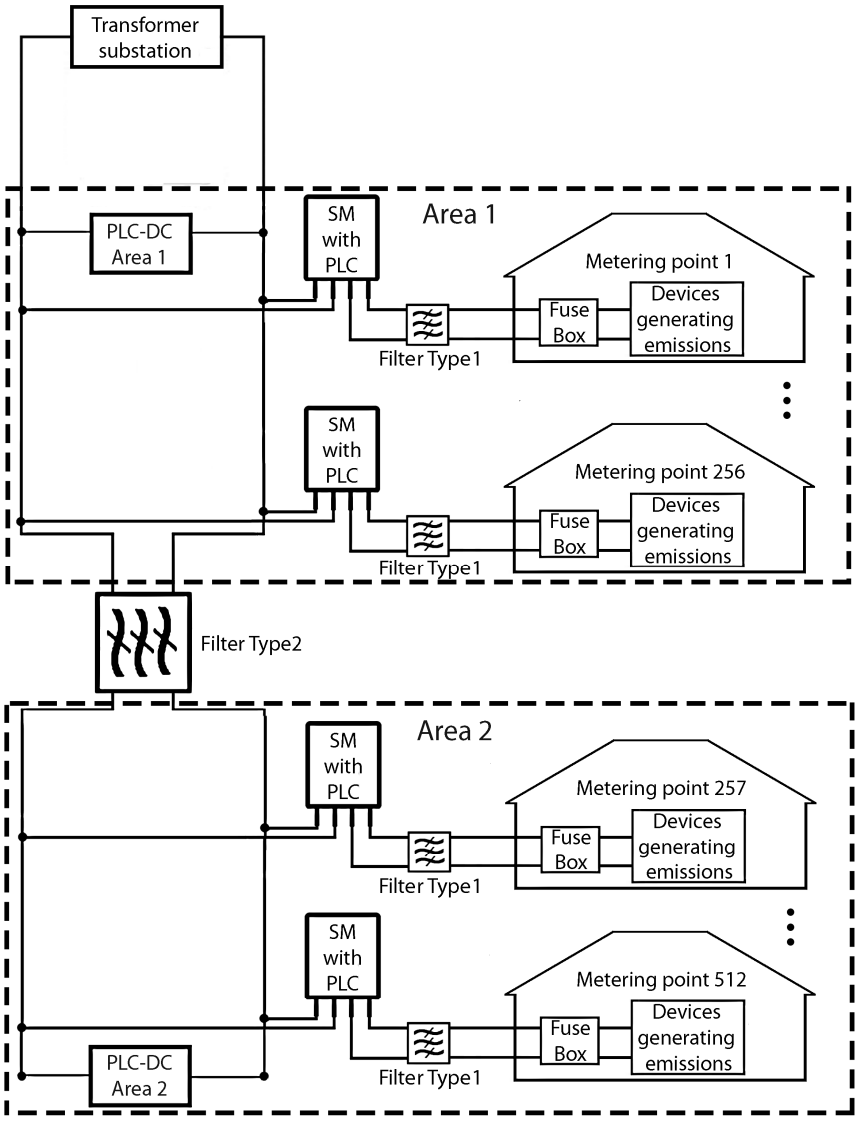

Figure 2. PLC filters use cases in the smart grid.

2.2. General Topolgies of Powerline Filters

In terms of the safety rating (leakage current) and insertion loss, both are two topologies of PLC filters with and without Y capacitors, namely C_y, having a middle point connected to protective earth [21]; these types of filters are shown in Figure 3. All other types of passive filters are different arrangements starting from these two types of filters. The graph in Figure 4 shows the insertion loss (with symmetrical loading) of the two filters depicted in Figure 3, as simulated using SPICE (Simulation Program with Integrated Circuit Emphasis). The optional resistor has the function to dampen oscillations at resonant frequencies and to discharge the capacitors.

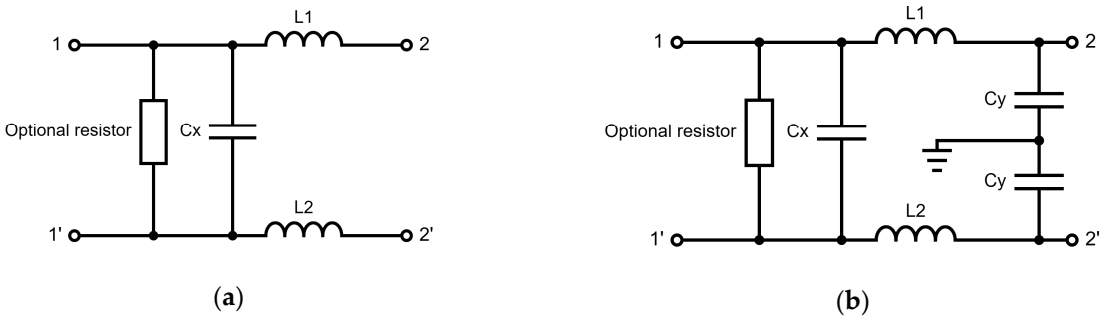

Figure 3. Basic types of filters: (**a**) PLC filter without a Y capacitor and (**b**) PLC filter with a Y capacitor.

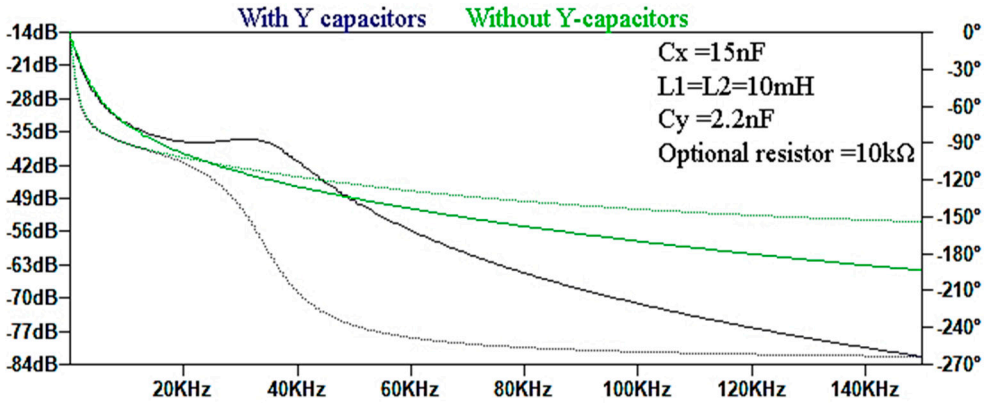

Figure 4. PLC filters' insertion loss and SPICE simulation.

2.3. Services Present in the Power Grid

The below-mentioned features present in the grid should not be affected if a PLC filter is fitted in the installation.

2.3.1. Residual Current Protective Devices

RCD (residual current protective device) is used in the installation as a protective device against faulty devices or the carelessness of users [30]. The tripping current of an RCD is $I_{\Delta n} \leq 30$ mA, which can be an issue in the case of a PLC filter with a leakage current being installed after the main fuse. Of course, the tripping current can be adjusted in some RCDs but the leakage of the Y capacitors might change due to capacitor ageing causing the RCD to trip unreliably.

2.3.2. Ripple Control System

Ripple control systems are devices used by the grid operator for load switching. Ripple control receivers are components of a system of remote control permitting the simultaneous switching of many loads from a central point. For the system to function it is necessary that the signal arrives from the injection point to the receiver sites. The ripple control signal frequency band is between 110 Hz and 3000 Hz [31] so it might be easily filtered out by the PLC filter.

2.3.3. Remote Connection of the Disconnect Unit

Some SMs detect the state of the main fuse when the power supply is disconnected from the SM disconnect unit. This feature is used to remote close the disconnect unit of the SM by cycling the main fuse off and on so that the energy supply to the customer is reestablished. The feature can be affected by the PLC filter in case it is fitted between the

SM and fuse box [32–34]. There is no description of the way this feature is implemented but it requires signal injection and measurement, which may be affected when using a PLC filter.

3. Filter Performance Measurement

This section presents the performance tests that should be performed as part of the benchmarking: insertion loss, PLC signal filtering, and impedance measurement.

3.1. Insertion Loss

In laboratory environments, the most straightforward method of testing the filters is by measuring its insertion loss (transfer function) using a VNA (vector network analyzer) [22] or an FRA (frequency response analyzer). In general, an FRA will allow lower frequency measurements and are robust to use in conjunction with power line couplers. Figure 5 is an offline insertion loss measurement setup [35] and Figure 6 is an online impedance measurement setup which uses line couplers [36], AC power supply, and load impedance. The practical implementation of the test setup from Figure 6 can be challenging due to non-standardized power supply impedance Z_S and load impedance Z_L values at PLC communication frequencies.

Passive impedance matching circuits can be used to measure the insertion loss of the filter when the impedance is different to 50 Ω. The main problem of passive impedance matching circuits is that the impedance matching is achieved only at a certain frequency; hence, to obtain a proper insertion loss with impedances different to 50 Ω, several matching circuits should be used. Another way of performing non-50 Ω measurements is to use matching transformers also known as baluns [37,38]. Some of the FRA models available on the market have separate ports for measuring and injecting the signal to the DUT (device under test) [39] so that an impedance matching circuit is not needed and the results with loading impedances different to 50 Ω are properly measured.

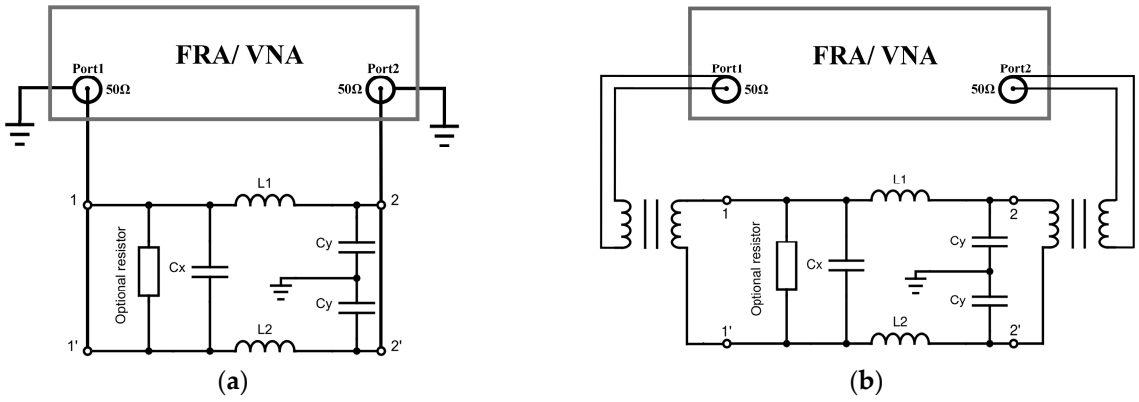

Figure 5. PLC filter offline insertion loss measurement setup. (**a**) Common mode measurement and (**b**) differential mode measurement.

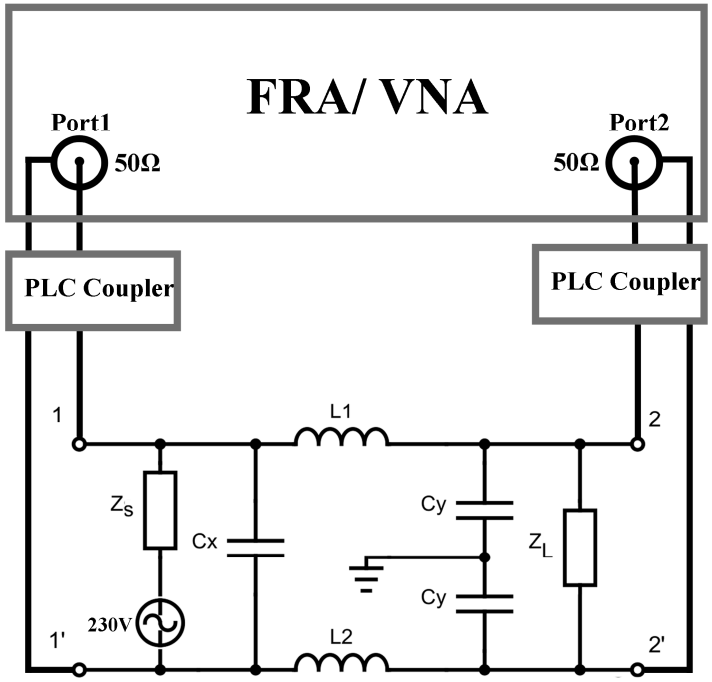

Figure 6. PLC filter online insertion loss test setup version 1.

In order to provide a controlled input impedance and noiseless power supply, a line impedance stabilization network (LISN) and two PLC couplers were used. The test setup from Figure 7 is derived from PLC and EMC standards [17,40] and it has the following features:

- Isolated AC power supply (isolation transformer);
- Symmetrical V-LISN that allows symmetrical measurements on phase and neutral; the unused half of the LISN is terminated with 50 Ω;
- Z_{in} and Z_L can be adjusted in order to obtain the required impedance at the port of the filter.

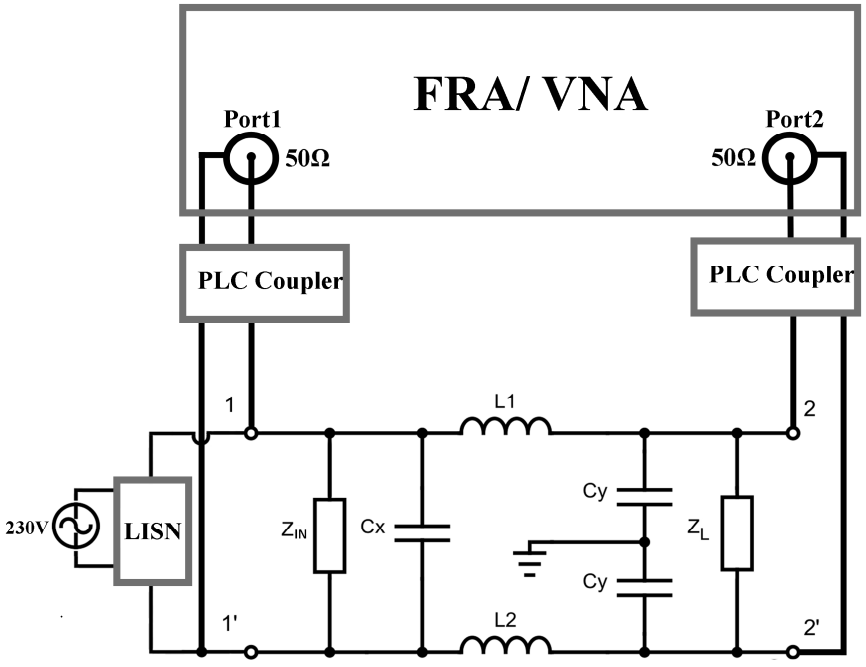

Figure 7. PLC filter online insertion loss test setup version 2.

Power line impedances encountered in real situations are 4 to 15 times lower than those of commercially available LISN. Figure 8 graphically presents the impedance from 20 kHz to 150 kHz of an 50 Ω/50 µH + 5 Ω LISN [40] and the power line impedance measured experimentally in five field condition cases [41–45].

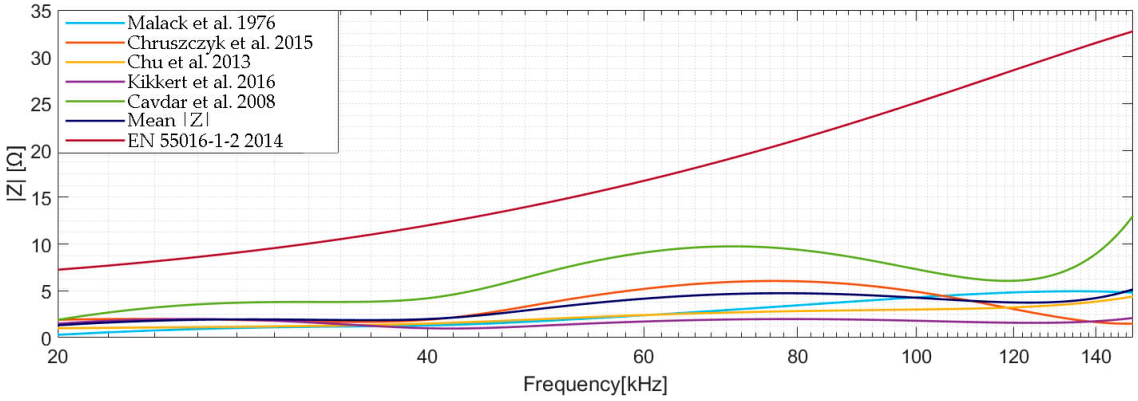

Figure 8. Power line impedance measurements compared to LISN impedance [40–45].

The adaptive impedance circuit from Figure 9 can be used to introduce Z_{in} and Z_L closer to values encountered in field conditions [46]. Figure 10 plots the impedance $|Z|$ and phase shift φ of half of the circuit (between L' and PE or N' and PE) from Figure 9; ideal components were used in the SPICE simulation.

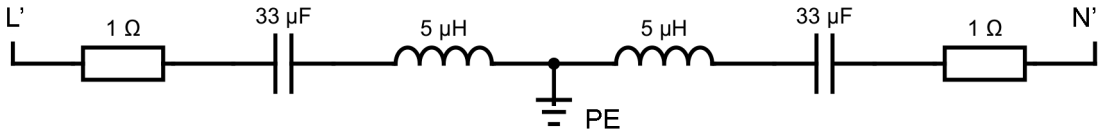

Figure 9. Adaptive impedance circuit for Z_{in} and Z_L.

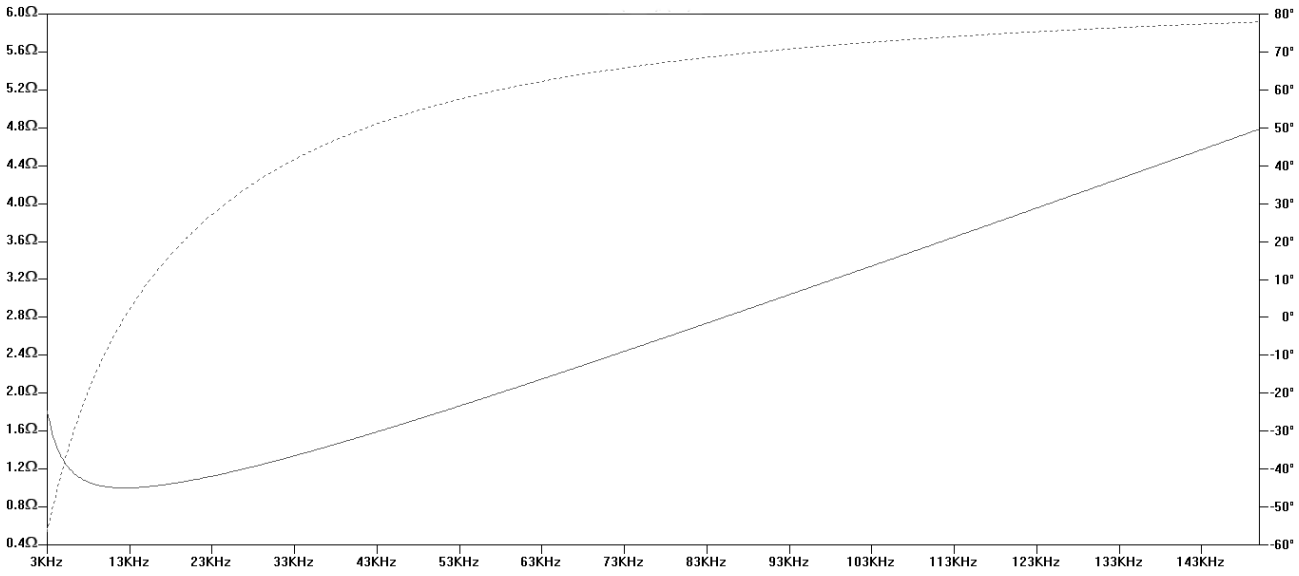

Figure 10. Impedance and phase plot for half of the adaptive impedance circuit.

The power consumption at the mains frequency f = 50 Hz of the adaptive impedance circuit from Figure 9 is P ≈ 1 kW and thus much lower compared to the power consumed

if a purely resistive 2 Ω load is used, P = 26.45 kW. The power consumption computations are detailed in Equations (1)–(11).

$$Z = \sqrt{R^2+(X_L - X_C)^2} \quad (1)$$

$$R = 1\ \Omega \quad (2)$$

$$X_L = 2\ \pi\ \mathrm{fL} = 1.5\ \mathrm{m\Omega} \quad (3)$$

$$X_C = \frac{1}{2\ \pi\ \mathrm{fC}} = 95.5\ \Omega \quad (4)$$

$$Z = 95.5\ \Omega \quad (5)$$

$$\varphi = \tan^{-1}\left(\frac{X_L - X_C}{R}\right) = -25.5^{\circ} \quad (6)$$

$$\cos\varphi = 0.9 \quad (7)$$

$$I_{RMS}/_2 = \frac{V_{RMS}/_2}{Z} = \frac{115}{95.5} = 1.2\ \mathrm{A} \quad (8)$$

$$P_{1/2\ adaptive\ circuit} = U_{RMS} I_{RMS} \cos\varphi = 230 \times 2.4 \times 0.9 = 496.8\ \mathrm{W} \quad (9)$$

$$P_{adaptive\ circuit} = 2 * P_{1/2\ adaptive\ circuit} = 992\ \mathrm{W} \quad (10)$$

$$P_{2\Omega\ Load} = \frac{U_{RMS}^2}{R} = \frac{52900}{2} = 26.45\ \mathrm{kW} \quad (11)$$

The online insertion loss test setup version 2 with Z_{in} and Z_L close to power line impedance replicates realistic power grid conditions, thus offering an accurate way of evaluating the PLC filters [47,48].

3.2. PLC Signal Filtering

In some use cases such as the filter, by separating two areas of the PLC system (Figure 2) the filter must block the PLC signal.

In the absence of an FRA or VNA there are two pragmatic ways of testing the PLC filters:

- Use PLC modems connected before and after the filter and measure the frame error rate, as shown in Figure 11;
- Configure a PLC modem in transmit mode and measure the signal level with a spectrum analyzer before and after the filter, as shown in Figure 12.

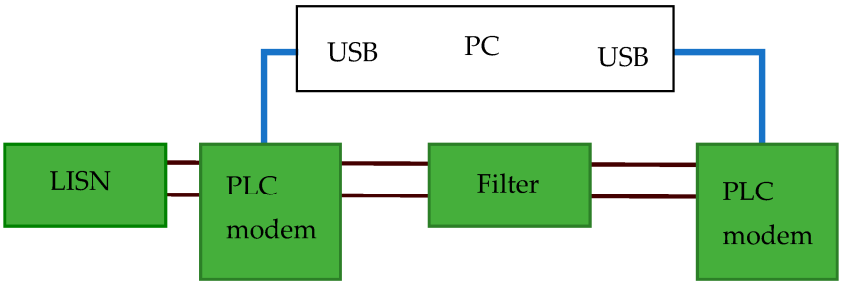

Figure 11. PLC signal filtering capability test setup version 1.

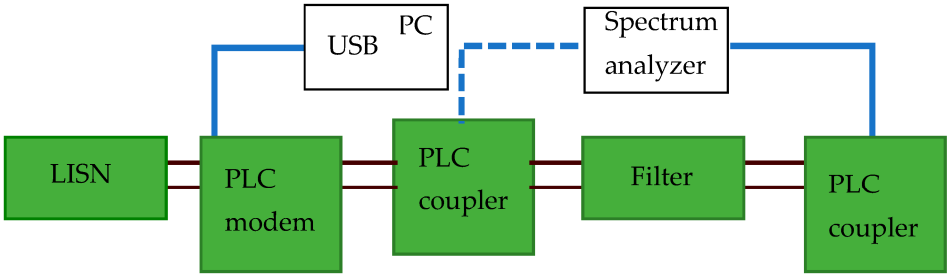

Figure 12. PLC signal filtering capability test setup version 2.

3.3. Impedance Measurement

The impedance of the filter should not affect the PLC modem performance. In some cases, the PLC filter is installed very close to the SM with a PLC modem, which can severely affect the transmitted and received signal. Higher filter input impedances can be achieved using higher order filters (multi-stage) such as the filter designed by us.

The most effective ways of measuring the impedance of the filter at PLC frequencies are:

- Offline measurement using the RLC meter, impedance analyzer, or VNA, Figure 13a;
- Online measurement using the impedance analyzer measuring method [49], Figure 13b;
- Online measurement using the voltage ratio method [49], Figure 13c;
- Offline measurement and monitoring of the voltage and current consumption of the PLC modem while transmitting carrier frequencies, Figure 13d.

Single port measurements with a VNA are not reliable at extreme impedance values (i.e., <1 Ω). The single port measurement limitation (S11) comes from the fact that the VNA is designed to measure the incident wave (E^+) entering the DUT (device under test) and the reflected wave(E^-) on impedances close to 50 Ω [50–52]. The ratio of these two waves is called the reflection coefficient (Γ) and it is used to compute the impedance of the DUT Z_L. The resolution of a VNA is not high enough for single port measurements at extreme impedance values: when Z_L is very low, Γ becomes close to −1, and when Z_L is very high, Γ becomes close to +1.

$$\Gamma = \frac{E^-}{E^+} = \frac{Z_L - 50}{Z_L + 50} \quad (12)$$

$$Z_L = 50\frac{(\Gamma + 1)}{(\Gamma - 1)} \quad (13)$$

In order to overcome the limitations of the single port measurements, the 2-Port VNA measurement technique can be used which is the equivalent of the 4-wire Kelvin DC technique for measuring resistance. Port 1 is used to inject to the DUT and port 2 is used to measure the voltage drop on the DUT.

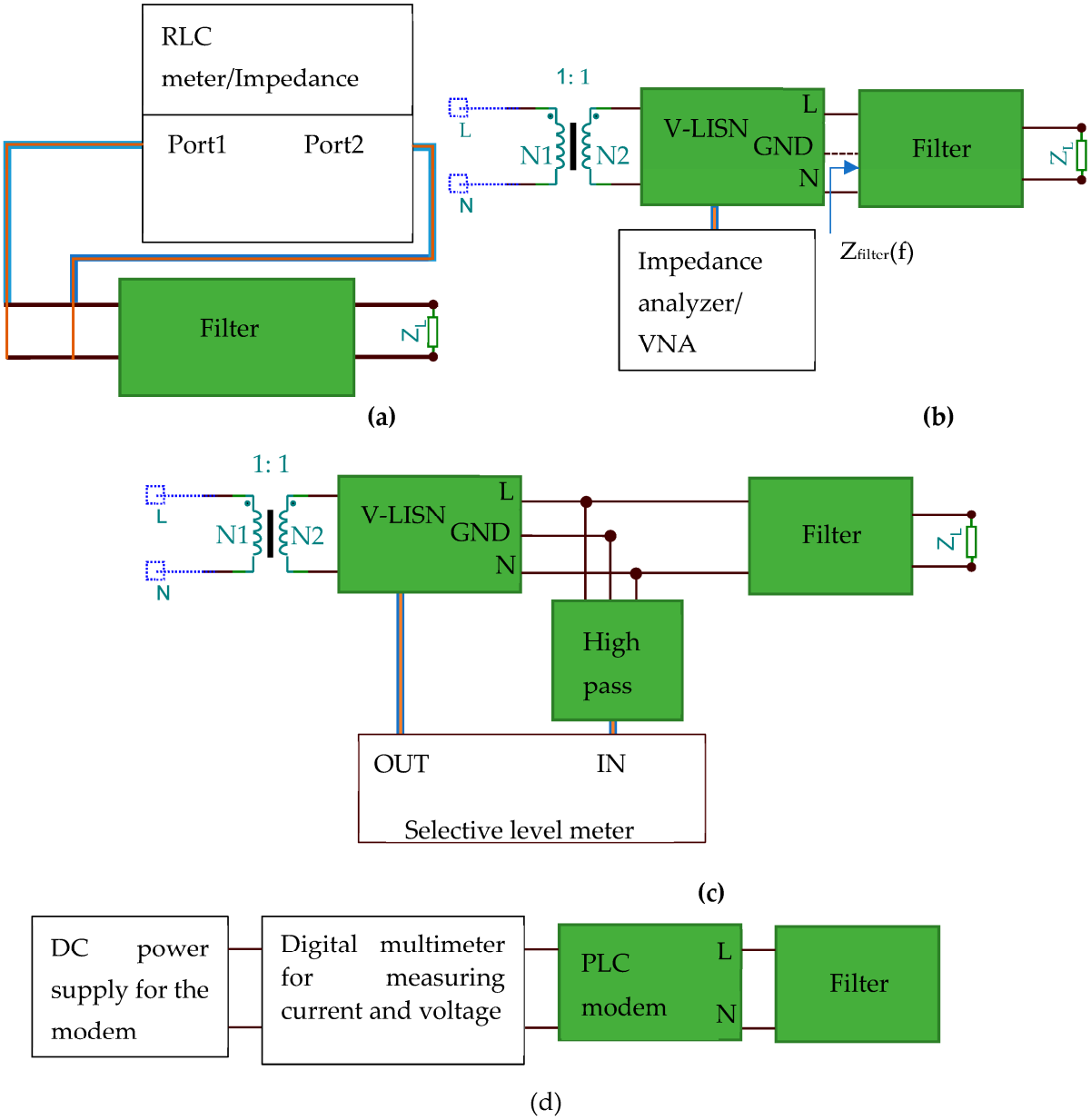

Figure 13. Impedance measurement: (**a**) offline measurement; (**b**) online measurement with an impedance analyzer; and (**c**) online measurement using the voltage ratio method and selective level meter. (**d**) Offline measurement and monitoring the voltage and current consumption of the PLC modem.

4. Additional Testing

This section presents the safety and immunity tests that should be performed as part of benchmarking in addition to the passive filter standard [28]: heating, surge, overcurrent, and short circuit.

4.1. Heating

Under maximum rated operating conditions, the housing of the filter shall not reach a temperature, which might cause a fire hazard or influence the filter and devices surrounding the filter.

The test can be performed by inspecting the filter with the thermal view camera [23] while maximum current passes through the filter. Given that the filter may be installed under similar conditions as the SM, it is important to test it accordingly [53]:

- The filter should carry the rated maximum rated current and voltage for 2 h;
- The temperature rise of the external surface should not exceed 65 °C, with an ambient temperature of 40 °C.

4.2. Surge

The test should be carried out according to the relevant surge testing standard [54] under the following conditions:

- Filter operating condition: circuits should be energized with reference voltage +5% without any load connected to the output of the circuit;
- Cable length between the surge generator and filter: 1 m;
- Tested in differential mode (line to line) and, if ground connection is available, common mode (line/neutral and ground);
- Phase angle: pulses to be applied at 60° and 240° relative to the zero crossing of the mains supply;
- Test voltage on the mains lines: 4 kV;
- Generator source impedance: 2 Ω;
- Number of pulses: five positive and five negative;
- Repetition rate: maximum 1/minute.

4.3. Overcurrent

It is recommended to conduct this test if there is no fuse fitted before the filter; this is the case when the filter is separating the two areas of the PLC grid as shown Figure 2. The filter shall be able to carry a short time overcurrent of 30 times the maximum rated current for one half-cycle at a rated frequency [55]. No degradation of the filter characteristics should be observed after this test.

4.4. Short Circuit

The short circuit condition can be simulated by short-circuiting the output of the filter and feeding the input with two times the maximum rated current until the filter will result in an open circuit. During testing, the filter should not be in an unsafe condition and after the test it should result in an open circuit.

4.5. Overvoltage

This test simulates the overvoltage that may occur in the grid due to faults such as earth fault, phase reversal, and voltage unbalances. All of the overvoltage conditions translate in an increased line or phase voltage. The most extreme case that can occur in a system having V_{L-N} = 230 V as the phase voltage is described below [55,56]:

$$V_{(L-N)nominalmax} = 1.1 \times 230V = 253V \quad (14)$$

$$V_{(L-L)max} = \sqrt{3} \times V_{(L-N)nominalmax} = 438V \quad (15)$$

5. PLC Filter Design, Simulation, and Evaluation

This section presents the design, simulation, and evaluation of the passive PLC filter.

5.1. PLC Filter Design

The filter was designed using the following requirements:

- The filter should reach −120 dB attenuation at 50 kHz because the maximum PLC signal level is 120 dBuV [16], thus blocking PLC signal passing through the filter;
- Filter power consumption at the mains frequency should be kept as low as possible;
- The filter saturation current should be at least 30 A, making it suitable for installation between SM and electrical installation of the building (i.e., main fuse);

- The filter input/output impedance in the NB-PLC frequency band must be as high as possible so that it does not affect the communication. As a minimum requirement, the impedance must be above 2 Ω because the PLC modems are designed and tested to transmit on 2 Ω loads [16];
- The filter design and component selection shall be conducted in order to ensure compliance with the tests described in Section 4 for additional testing.

We have designed the 13th order filter from Figure 14 in compliance with the requirements from the beginning of this section. The compliance and performance have been assessed in Section 5.3.

Electronic component selection has an important role in the implementation of the filter, Table 1 is the bill of materials explaining our selection.

Table 1. Filter comparison based on datasheet values.

Component(s)	Part Descriptions and Use Case Explanation
TMOV	The filter incorporates a TMOV (thermally protected metal oxide varistor) from Little Fuse™ TMOV20RP460E [57]. The TMOV compared to traditional metal oxide varistors provides surge protection while ensuring that it will not conduct at a main voltage, thus overheating and ultimately catching fire [58]. The selected TMOV will start conducting at 460 V, thus safe operation of the filter is ensured during overvoltage $V_{(L-L)max} = 438$ V.
R1, R2 and R3	An array of three series connected resistors is used for passive damping of oscillations that might occur in the grid [59]. Surge safety resistors SSR300J10K0TKZTB500 from Firstohm™ [60] were chosen. Series connection is preferred in order to ensure that there is no arching due to insufficient clearance and creepage distances [61].
C1 and C5	Polyester film capacitors capable of withstanding $V_{(L-L)max} = 438$ V were used. Specifically in our design, JGGC series from JB® [62] were used.
L1 to L8	The inductors were designed and built using a toroidal core made out of Sendust MS-184075-2 [63] manufactured by Micrometals™. Sendust is appropriate to be used in applications requiring high permeability, low coercivity, high resistivity, and high magnetization, such as inductors used in filtering applications [64]. In order to obtain L = 100 μH and a current rating of 40A, N = 26 turns of 4mm² stranded wire are used.
C2, C3, C4	Polyester film capacitors capable of withstanding $V_{(L-L)max} = 438$ V were used. Specifically in our design, JGGC series from JB® [62] were used. The value of the capacitors was adjusted to C = 2.2 μF based on simulation and calculation values in order to have a trade-off between power consumption, attenuation, and input/ output impedance.

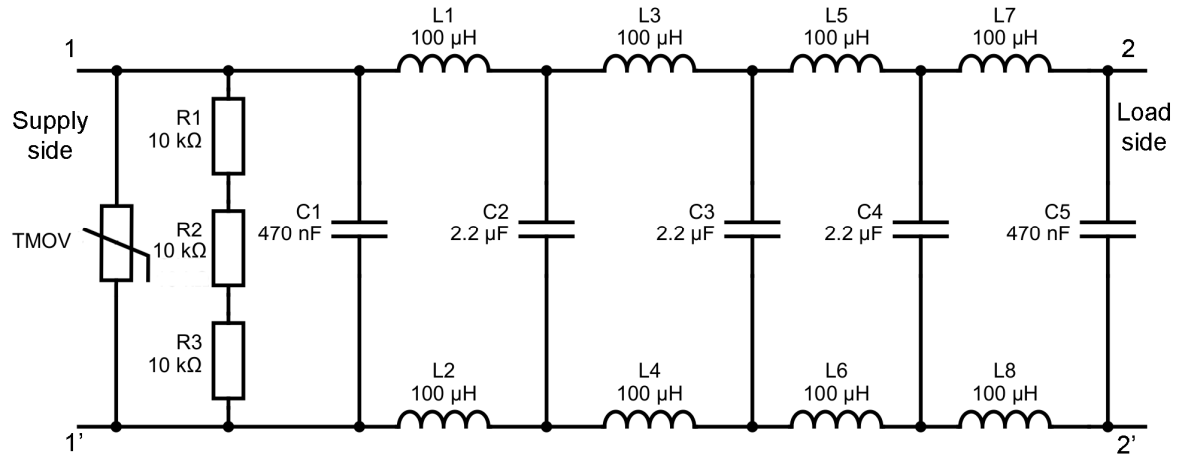

Figure 14. Designed PLC filter.

5.2. PLC Simulation Using the S-Parameters Simulator

S11 parameters for each component were measured using a VNA and the obtained Touchstone files [65] are used in simulating the filter in the RFSim99 S-Parameters simulator. RFSim99 is a linear S-parameter-based circuit simulator which solves matrix equations for two-port devices.

Figure 15 is the graphical representation of a two-port network [66,67]:

- a_1 and a_2 are the incident waves for Port1 and Port2;
- b_1 and b_2 are the reflected waves for Port1 and Port2;
- S_{21} is the forward transmission coefficient (from port 1 to port 2) and S_{12} is the reverse transmission coefficient (from port 2 to port 1);
- S_{11} is the input reflection coefficient and S_{22} is the output reflection coefficient.

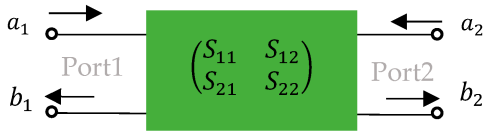

Figure 15. Generalized two-port network.

Below is the matrix algebraic representation of two port S-parameters [66,67] which is also used by the simulator:

$$S_{11} = \frac{b_1}{a_1} \tag{16}$$

$$S_{12} = \frac{b_1}{a_2} \tag{17}$$

$$S_{21} = \frac{b_2}{a_1} \tag{18}$$

$$S_{22} = \frac{b_2}{a_2} \tag{19}$$

$$\begin{pmatrix} b_1 \\ b_2 \end{pmatrix} = \begin{pmatrix} S_{11} & S_{12} \\ S_{21} & S_{22} \end{pmatrix} \times \begin{pmatrix} a_1 \\ a_2 \end{pmatrix} \tag{20}$$

For the measurements, PLC filter online insertion loss test setup version 2, shown in Figure 7, was utilized. The actual implementation of the test setup is depicted in Figure 16.

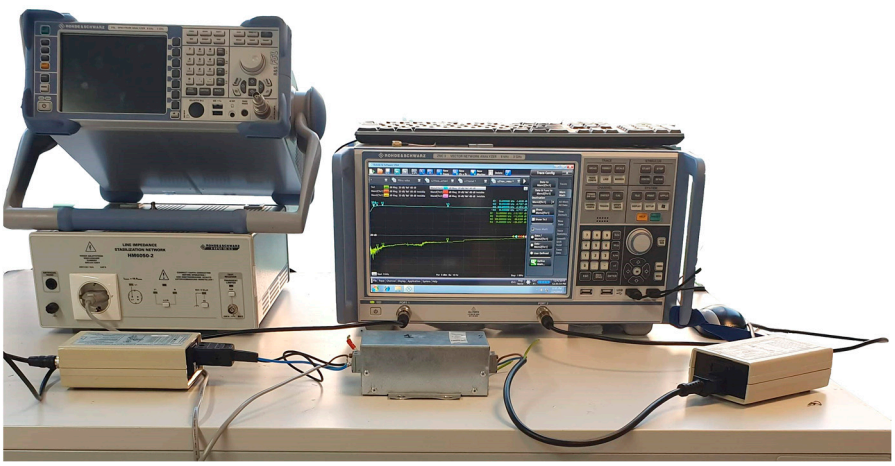

Figure 16. PLC filters online insertion loss test setup version 2 measurements.

Figure 17 presents the results of the simulated and measured insertion loss for the proposed filter.

Measurements and graphical representation were performed with the following settings and conventions:

- Measurement equipment reference impedance: $Z_0 = 50\ \Omega$;
- The measured S21 [dB] parameter is considered to be the insertion loss of the filter [68];
- Due to the dynamic range and noise floor of the VNA, measurements can be performed starting low at −130 dB [69]. Although the simulated S21 magnitude values are as low as −300 dB, all magnitude values ≤−140 dB were scaled to −140 dB in order to facilitate graphical representation.

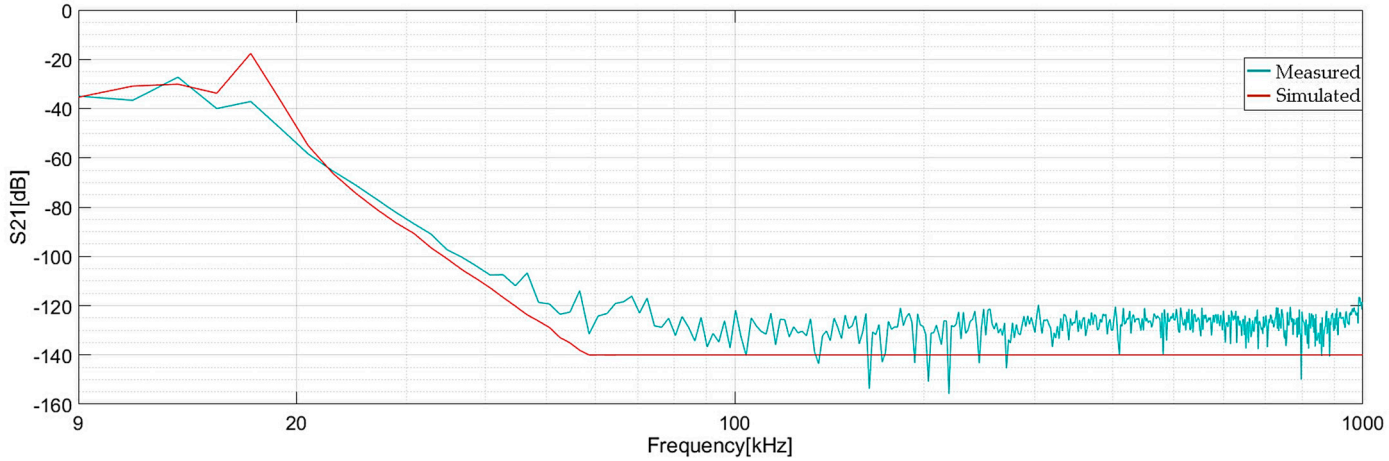

Figure 17. Comparison between measured and simulated insertion loss.

5.3. Proposed Filter Evaluation and Comparison to Other Commercially Available Filters

The filter proposed in Figure 14 is evaluated and compared to other filters advertised as for PLC and with similar characteristics to the proposed filter. The evaluation is performed according to a part of the test methods described above. In order to prevent product biasing, the filter manufacturers and manufacturer part numbers are anonymized; however, the schematic of the benchmarked filters together with the component values are shown in Section 5.3.1.

5.3.1. PLC Filter Insertion Loss and Power Consumption Measurements

Insertion loss measurements were performed in the following conditions:

- The test setup used is the PLC filter online insertion loss test setup 2 shown in Figure 7;
- The first step is to validate the test setup by directly connecting the PLC couplers to one another. The setup validity check is named “PLC Couplers” in the below figures;
- The subsequent actions involve conducting measurements while the filter is installed, considering three different states: no mains voltage named “Unenergised”, mains voltage named “Energised”, and a 2000 W load with the mains voltage named “Energised with 2000 W load”. The naming convention utilized in the figures below, which display the results of insertion loss measurements, remains consistent.

Figure 18 presents the insertion loss of the proposed filter.

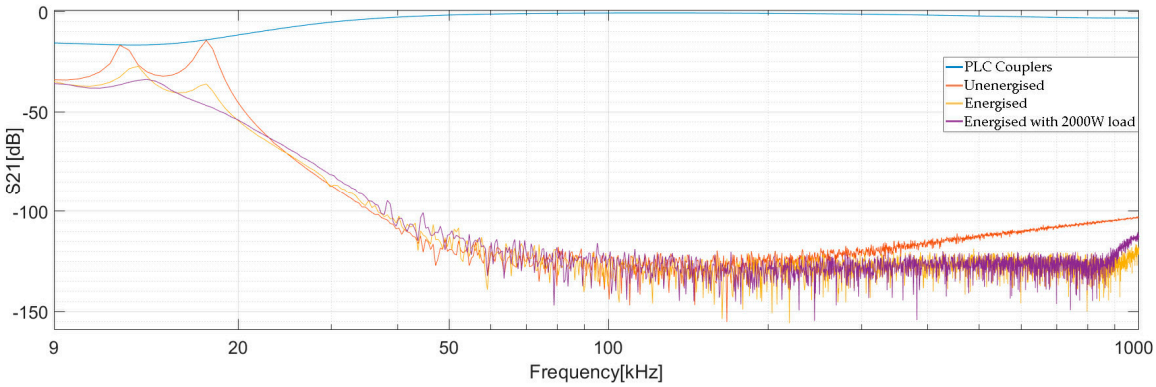

Figure 18. Proposed filter insertion loss measurement using PLC filter online insertion loss test setup version 2.

Figure 19 shows the schematic extracted from the datasheet of Filter 1. During measurements, the ground connection of the Y-capacitors between C2 and C3 was left floating and thus the filter was connected in the same way as an eighth-order passive filter or a two-stage filter from Figure 3b. Figure 20 presents the insertion loss of filter 1.

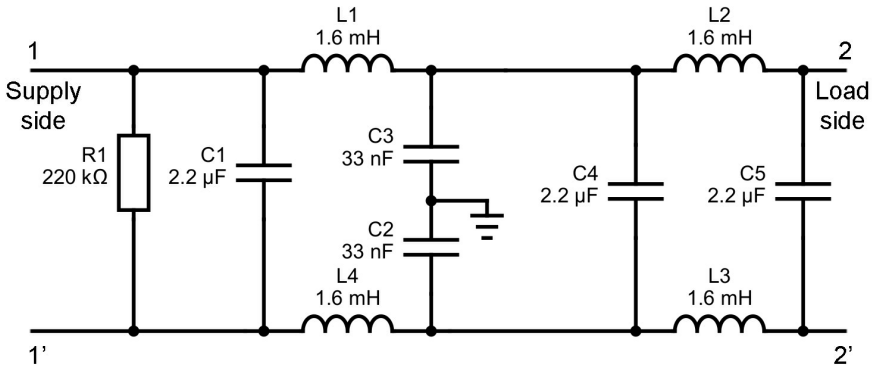

Figure 19. Filter 1 schematic.

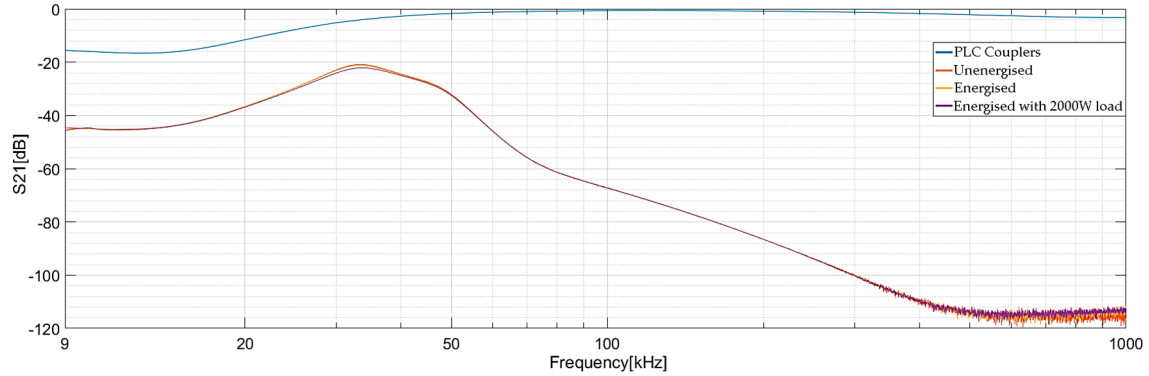

Figure 20. Filter 1 insertion loss measurement using PLC filter online insertion loss test setup version2.

Figure 21 shows the reverse-engineered schematic of Filter 2 (the schematic was not available in the datasheet). The filter is a resonant type of filter with a resonance frequency between 20 kHz and 30 kHz, this is also visible in Figure 22 where the attention S21 [dB] has its minimum value. These types of filters have the disadvantage that the attenuation is highly dependent on the input and output resistance. Proof of this statement entails the huge difference in attenuation (10 dB to 40 dB) from Figure 22 between the attenuation

when the filter is energized (no load) and the case when the filter has a 2000 W load. Figure 22 presents the insertion loss of filter 2.

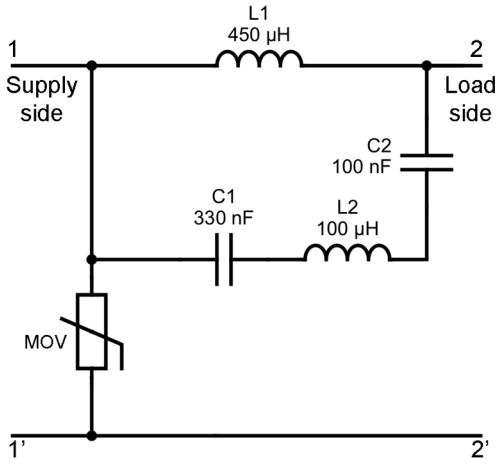

Figure 21. Filter 2 schematic.

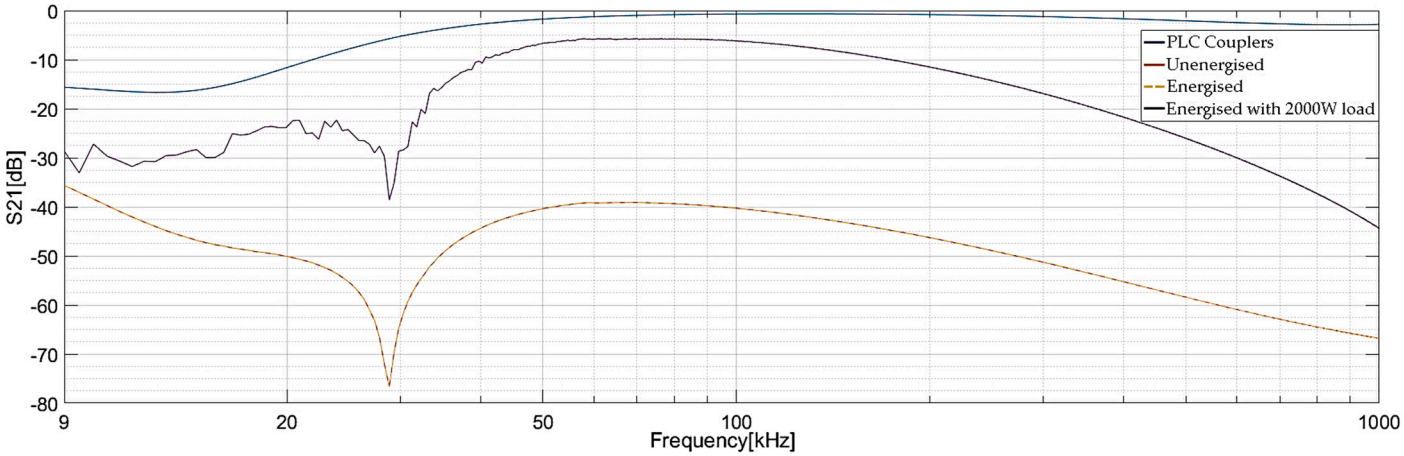

Figure 22. Filter 2 insertion loss measurement using PLC filter online insertion loss test setup version 2.

Figure 23 shows the schematic extracted from the datasheet of Filter 3 which is a sixth order passive filter. Figure 24 presents the insertion loss of filter 3.

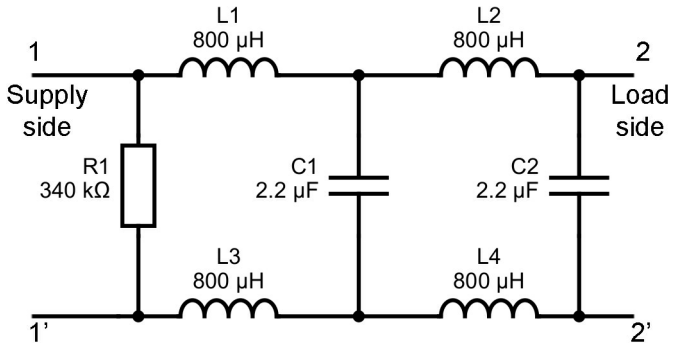

Figure 23. Filter 3 schematic.

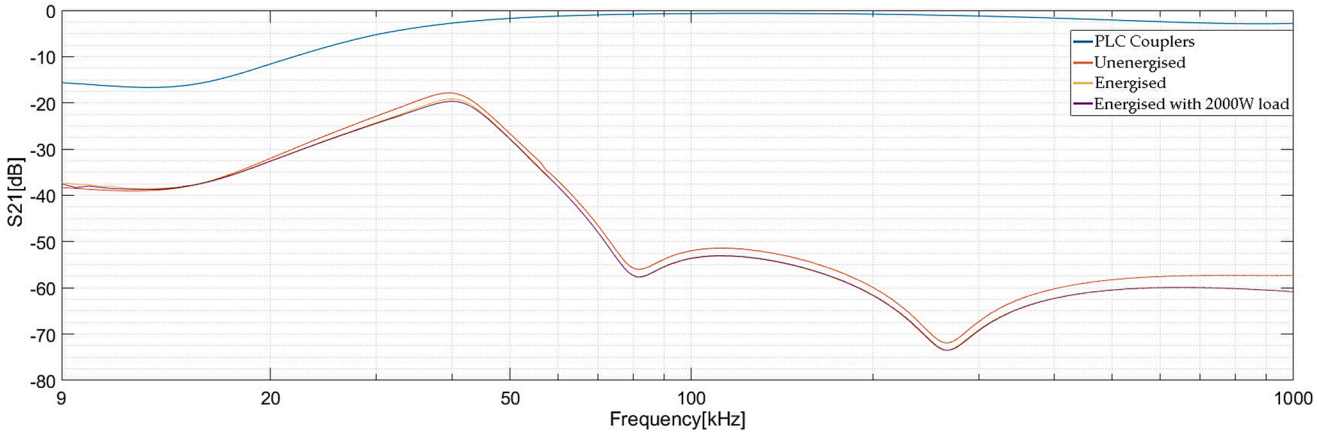

Figure 24. Filter 3 insertion loss measurement using PLC filter online insertion loss test setup version 2.

Table 2 summarizes the results of the insertion loss measurements and power consumption measurements while comparing them to datasheet values. The rated current value is written in the table as a similarity reference between the filters.

The data from Table 2 are obtained from below methods and sources:

- Power consumption measurements at 230V 50Hz;
- Insertion loss extracted from measurement results is shown in Figures 18, 20, 22, and 24;
- Insertion loss gap measurement using PLC signal filtering capability test setup version 1 is shown in Figure 11. These measurements reflect the gap between the filter attenuation and the attenuation at which the communication stops.

Table 2. Filter comparison based on measured and datasheet values.

Filter Number	Rated Current [A]	Power Consumption [W]	Insertion Loss [dB] at 50 kHz		Insertion Loss Gap for Blocking the PLC Communication [dB]
			Datasheet Value	Measured Value Filter Energized with 2000 W Load	
Proposed filter	30 *	0.597	−130 *	−120	0
Filter 1	25	0.524	−40	−32	53
Filter 2	45	0.033	−40	−7	59
Filter 3	25	0.215	−20	−28	55

* Designed and simulated value.

The filter developed in this study exhibits exceptional features, including the best insertion loss versus frequency, a three-fold increase in attenuation at 50 kHz (−130 dB) in comparison to the best commercially available filter (−40 dB), and a power consumption of 0.6 W, similarly to the most power-efficient commercial filter (0.5 W). Furthermore, it has the second-best input and output impedance of 3.6 Ω within the frequency range of 35 kHz–95 kHz.

5.3.2. PLC Filter Impedance Estimation

Table 3 summarizes the PLC modem current consumption in transmit mode (sending frequency beacons in 35 kHz–95 kHz) while being connected in turns at the input and output of the filter. The filter impedance estimation method is shown in Figure 13d.

The measured modem's power consumption is 0.42 A when transmitting over a resistive impedance of 1 Ω.

Table 3. Modem power consumption and estimated impedance in the frequency range 35–95 kHz.

Filter Number and Location	Current Consumption RMS [A]	Estimated Impedance [Ω]
Proposed filter output	0.125	3.36
Proposed filter input	0.125	3.36
Filter 1 output	0.275	1.53
Filter 1 input	0.275	1.53
Filter 2 output	0.025	16.8
Filter 2 input	0.075	5.6
Filter 3 output	0.225	1.87
Filter 3 input	0.205	2.05

6. Conclusions and Future Work

In conclusion, this paper has presented comprehensive benchmarking, design methods, and actual measurements for the development and evaluation of power line filters, with a specific focus on the CENELEC A communication band.

We have designed a power line filter using an S-parameters simulator and real passive components and detailed information regarding the component selection and filter construction has been provided. Practical validation of the simulated values was achieved through actual measurements. Benchmarking against three commercially available filters shows that our filter is the best suited for filtering below 150 kHz.

Our filter has superior characteristics, such as the best insertion loss versus frequency, three times higher attenuation at 50 kHz (−130 dB) compared to the best commercially available filter (−40 dB), and a power consumption of 0.6 W which is comparable to the most power-efficient commercial filter (0.5 W). Additionally, our filter has the second-best input and output impedance of 3.6 Ω within the frequency range of 35 kHz–95 kHz.

The proposed filter has the maximum rated current limit of only 30 A, which makes it suitable as a type 1 filter but unsuitable as a type 2 filter (separating two sections of the power grid) as defined per Section 2.1. It is of interest to design a type 2 filter using the design methods presented in this paper.

As future work, we propose to benchmark additional power line filter using the test methods presented in Sections 3 and 4. In addition, it is of interest for us to design and evaluate a hybrid between resonant and *n*th order filters with the scope of reducing the order of the filter while maintaining the attenuation below 150 kHz.

Author Contributions: Conceptualization, S.A. and R.V.; Methodology, S.A. and R.V.; Resources, S.A. and R.V.; Validation, S.A.; Writing—original draft, S.A.; Writing—review and editing, S.A. and R.V. All authors have read and agreed to the published version of the manuscript.

Funding: This research received no external funding.

Institutional Review Board Statement: Not applicable.

Informed Consent Statement: Not applicable.

Data Availability Statement: Not applicable.

Conflicts of Interest: The authors declare no conflict of interest.

References

1. Vitiello, S.; Andreadou, N.; Ardelean, M.; Fulli, G. Smart Metering Roll-Out in Europe: Where Do We Stand? Cost Benefit Analyses in the Clean Energy Package and Research Trends in the Green Deal. *Energies* **2022**, *15*, 2340. https://doi.org/10.3390/en15072340.
2. Directorate-General for Energy (European Commission); Tractebel Impact; Alaton, C.; Tounquet, F. *Benchmarking Smart Metering Deployment in the EU-28: Final Report*; Publications Office of the European Union: Luxembourg, 2020; ISBN 978-92-76-17295-6.

3. AMI and Power Line Communications. Available online: https://www.networkedenergy.com/en/news-events/ami-and-power-line-communications (accessed on 29 January 2023).
4. Bartak, G.F.; Abart, A. EMI in the Frequency Range 2–150 KHz. In Proceedings of the International Symposium on Electromagnetic Compatibility, Tokyo, Japan, 12–16 May 2014; pp. 577–580.
5. Long, L.C.; Sayed, W.E.; Munesswaran, V.; Moonen, N.; Smolenski, R.; Lezynski, P. Assessment of Conducted Emission for Multiple Compact Fluorescent Lamps in Various Grid Topology. *Electronics* **2021**, *10*, 2258. https://doi.org/10.3390/electronics10182258.
6. Lodetti, S.; Gallarreta, A.; Ritzmann, D.; Khokhlov, V.; Wright, P.; Meyer, J.; Fernández, I.; de la Vega, D. On the Suitability of the CISPR 16 Method for Measuring Conducted Emissions in the 2–150kHz Range in Low Voltage Grids. *Electr. Power Syst. Res.* **2023**, *216*, 109011. https://doi.org/10.1016/j.epsr.2022.109011.
7. Gallarreta, A.; Fernández, I.; Ritzmann, D.; Lodetti, S.; Khokhlov, V.; Wright, P.; Meyer, J.; de la Vega, D. A Light Measurement Method for 9–150 KHz Disturbances in Power Grids Comparable to CISPR Quasi-Peak. *IEEE Trans. Instrum. Meas.* **2022**, *71*, 1–10. https://doi.org/10.1109/TIM.2022.3195255.
8. Garrido, J.; Moreno-Munoz, A.; Gil-de-Castro, A.; Pallares-Lopez, V.; Morales-Leal, T. Supraharmonics Emission from LED Lamps: A Reduction Proposal Based on Random Pulse-Width Modulation. *Electr. Power Syst. Res.* **2018**, *164*, 11–19. https://doi.org/10.1016/j.epsr.2018.07.032.
9. Girotto, M.; Tonello, A.M. EMC Regulations and Spectral Constraints for Multicarrier Modulation in PLC. *IEEE Access* **2017**, *5*, 4954–4966. https://doi.org/10.1109/ACCESS.2017.2676352.
10. Fernandez, I.; García, M.; de la Vega, D.; Arrinda, A.; Angulo, I.; Arzuaga, T.; Fernández, A. Characterization of Non Intentional Conducted Emissions Up to 500 KHz in Urban Environment. *REPQJ* **2018**, *1*, 663–668. https://doi.org/10.24084/repqj16.425.
11. Uribe-Pérez, N.; Angulo, I.; Hernández-Callejo, L.; Arzuaga, T.; De la Vega, D.; Arrinda, A. Study of Unwanted Emissions in the CENELEC-A Band Generated by Distributed Energy Resources and Their Influence over Narrow Band Power Line Communications. *Energies* **2016**, *9*, 1007. https://doi.org/10.3390/en9121007.
12. Szymczyk, C.; Nieß, C.; Bumiller, G. An On-Line Measurement Approach for EMI Filter Characterization. In Proceedings of the 2021 IEEE International Symposium on Power Line Communications and Its Applications (ISPLC), Aachen, Germany, 26–27 October 2021; pp. 90–95.
13. Fernández, I.; de la Vega, D.; Arrinda, A.; Angulo, I.; Uribe-Pérez, N.; Llano, A. Field Trials for the Characterization of Non-Intentional Emissions at Low-Voltage Grid in the Frequency Range Assigned to NB-PLC Technologies. *Electronics* **2019**, *8*, 1044. https://doi.org/10.3390/electronics8091044.
14. Fernandez, I.; Uribe-Pérez, N.; Eizmendi, I.; Angulo, I.; de la Vega, D.; Arrinda, A.; Arzuaga, T. Characterization of Non-Intentional Emissions from Distributed Energy Resources up to 500 kHz: A Case Study in Spain. *Int. J. Electr. Power Energy Syst.* **2019**, *105*, 549–563. https://doi.org/10.1016/j.ijepes.2018.08.048.
15. Sayed, W.E.; Lezynski, P.; Smolenski, R.; Moonen, N.; Crovetti, P.; Thomas, D.W.P. The Effect of EMI Generated from Spread-Spectrum-Modulated SiC-Based Buck Converter on the G3-PLC Channel. *Electronics* **2021**, *10*, 1416. https://doi.org/10.3390/electronics10121416.
16. *EN 50065-1:2011*; Signalling on Low-Voltage Electrical Installations in the Frequency Range 3 KHz to 148.5 KHz. General Requirements, Frequency Bands and Electromagnetic Disturbances. Available online: https://knowledge.bsigroup.com/products/signalling-on-low-voltage-electrical-installations-in-the-frequency-range-3-khz-to-148-5-khz-general-requirements-frequency-bands-and-electromagnetic-disturbances-1/standard (accessed on 2 April 2023).
17. *EN 55015:2013+A1:2015*; Limits and Methods of Measurement of Radio Disturbance Characteristics of Electrical Lighting and Similar Equipment. 2015. Available online: https://knowledge.bsigroup.com/products/limits-and-methods-of-measurement-of-radio-disturbance-characteristics-of-electrical-lighting-and-similar-equipment-1/standard (accessed on 22 April 2023).
18. *EN 55014-1:2017*; Electromagnetic Compatibility. Requirements for Household Appliances, Electric Tools and Similar Apparatus. Emission. Available online: https://knowledge.bsigroup.com/products/electromagnetic-compatibility-requirements-for-household-appliances-electric-tools-and-similar-apparatus-emission-2/standard (accessed on 22 April 2023).
19. Lin, J.; Magnago, F.; Alemany, J.M. Chapter 1—Optimization Methods Applied to Power Systems: Current Practices and Challenges. In *Classical and Recent Aspects of Power System Optimization*; Zobaa, A.F., Abdel Aleem, S.H.E., Abdelaziz, A.Y., Eds.; Academic Press: Cambridge, MA, USA, 2018; pp. 1–18; ISBN 978-0-12-812441-3.
20. Power Electronics: Circuits, Devices & Applications. Available online: https://www.pearson.com/en-us/subject-catalog/p/power-electronics-circuits-devices--applications/P200000003551/9780137982097 (accessed on 24 May 2023).

21. Tarateeraseth, V. EMI Filter Design: Part III: Selection of Filter Topology for Optimal Performance. *IEEE Electromagn. Compat. Mag.* **2012**, *1*, 60–73. https://doi.org/10.1109/MEMC.2012.6244975.
22. Varajão, D.; Esteves Araújo, R.; Miranda, L.M.; Peças Lopes, J.A. EMI Filter Design for a Single-Stage Bidirectional and Isolated AC–DC Matrix Converter. *Electronics* **2018**, *7*, 318. https://doi.org/10.3390/electronics7110318.
23. Bernacki, K.; Wybrańczyk, D.; Zygmanowski, M.; Latko, A.; Michalak, J.; Rymarski, Z. Disturbance and Signal Filter for Power Line Communication. *Electronics* **2019**, *8*, 378. https://doi.org/10.3390/electronics8040378.
24. Da Rocha Farias, L.; Monteiro, L.F.; Leme, M.O.; Stevan, S.L. Empirical Analysis of the Communication in Industrial Environment Based on G3-Power Line Communication and Influences from Electrical Grid. *Electronics* **2018**, *7*, 194. https://doi.org/10.3390/electronics7090194.
25. Vukicevic, A.; Bittner, M.; Rubinstein, A.; Rubinstein, M.; Rachidi, F. A Concept to Enhance System Data Rate for PLC Access Networks. In Proceedings of the 2008 IEEE International Symposium on Power Line Communications and Its Applications; Jeju, Republic of Korea, 2–4 April 2008; pp. 105–110.
26. Nemashkalo, D.; Moonen, N.; Leferink, F. Practical Consideration on Power Line Filter Design and Implementation. In Proceedings of the 2020 International Symposium on Electromagnetic Compatibility—EMC Europe, Rome, Italy, 23 September 2020; pp. 1–6.
27. Sekhar, P.C.; Gopal, Y.R. Design of S Parameters for Various Filters. Available online: https://www.semanticscholar.org/paper/DESIGN-OF-S-PARAMETERS-FOR-VARIOUS-FILTERS-Sekhar-Gopal/1d0e0e16c8a9b9952870902f67a64d3126efd4d7 (accessed on 22 April 2023).
28. *IEC 60939-3:2015*; Passive Filter Units for Electromagnetic Interference Suppression—Part 3: Passive Filter Units for Which Safety Tests Are Appropriate. Available online: https://knowledge.bsigroup.com/products/passive-filter-units-for-electromagnetic-interference-suppression-passive-filter-units-for-which-safety-tests-are-appropriate/standard (accessed on 22 April 2023).
29. Blocking Filter–Grupo Premo. Available online: https://www.grupopremo.com/content/102-blocking-filter (accessed on 12 May 2023).
30. *EN 61140:2016*; Protection against Electric Shock. Common Aspects for Installation and Equipment. 2016. Available online: https://knowledge.bsigroup.com/products/protection-against-electric-shock-common-aspects-for-installation-and-equipment/tracked-changes (accessed on 2 April 2023).
31. Toonen, J.; Bhattacharyya, S.; Cobben, S. Impacts of Ripple Control Signals at Low Voltage Customer's Installations. In Proceedings of the 22nd International Conference and Exhibition on Electricity Distribution (CIRED 2013); Stockholm, Sweden, 10–13 June 2013; Institution of Engineering and Technology: Stevenage, UK, 2013; p. 256.
32. Instruction Leaflet for the Linky Smart Meter Single-Phase Meter. Available Online: https://www.Enedis.Fr/Sites/Default/Files/Notice_compteur_Linky_Monophase_anglais.Pdf (accessed on 14 April 2023).
33. What to Do If Your Fuse Box Trips? Available Online: Https://www.Endesaclientes.Com/Blog/What-to-Do-Fuse-Box-Trips (accessed on 14 April 2023).
34. Instrucciones Para La Reconexión Del Interruptor de Control de Potencia (ICP). Available Online: Https://www.Iberdroladistribucion.Es/Socdis/Gc/Prod/Es_ES/Contenidos/Docs/Rearme_icp.Pdf (accessed on 14 April 2023).
35. TDK General Technical Information. Available Online: Https://www.Tdk-Electronics.Tdk.Com/En/155646/Tech-Library (accessed on 15 March 2023).
36. STEVAL-XPLM01CPL—Power Line Communication AC Coupling Circuit—STMicroelectronics. Available online: https://www.st.com/en/evaluation-tools/steval-xplm01cpl.html (accessed on 14 April 2023).
37. Theofylaktos, J.D.W.. *Calibration Procedure for Measuring S-Parameters in Balun Applications on 150-Ω High-Speed Cables*; National Aeronautics and Space Administration: Cleveland, OI, USA, 2012
38. Using Baluns and RF Components for Impedance Matching. Available online: https://www.coilcraft.com/pdfs/Doc1077_Baluns_and_Impedance_Matching.pdf (accessed on 22 April 2023).
39. SLM3505 User Manual. Available online: https://www.newtons4th.com/wp-content/uploads/2021/05/D000200-SLM3505-User-Manual-v3.0.pdf (accessed on 22 April 2023)..
40. *EN 55016-1-2:2014+A1:2018*; Specification for Radio Disturbance and Immunity Measuring Apparatus and Methods. Radio Disturbance and Immunity Measuring Apparatus. Coupling Devices for Conducted Disturbance Measurements. 2018. Available online: https://knowledge.bsigroup.com/products/specification-for-radio-disturbance-and-immunity-measuring-apparatus-and-methods-radio-disturbance-and-immunity-measuring-apparatus-coupling-devices-for-conducted-disturbance-measurements/standard (accessed on 4 April 2023).
41. Malack, J.A.; Engstrom, J.R. RF Impedance of United States and European Power Lines. *IEEE Trans. Electromagn. Compat.* 1976, *EMC-18*, 36–38. https://doi.org/10.1109/TEMC.1976.303453.

42. Chruszczyk, Ł. Low-Voltage Grid Impedance Measurements in 10 KHz–1 MHz Frequency Range. In Proceedings of the 2015 IEEE 3rd Workshop on Advances in Information, Electronic and Electrical Engineering (AIEEE), Riga, Latvia, 13–14 November 2015; pp. 1–6.
43. Chu, G.; Li, J.; Liu, W. Narrow Band Power Line Channel Characteristics for Low Voltage Access Network in China. In Proceedings of the 2013 IEEE 17th International Symposium on Power Line Communications and Its Applications, Johannesburg, South Africa, 24–27 March 2013; pp. 297–302.
44. Kikkert, C.J.; Zhu, S. Resistive Shunt On-Line Impedance Analyzer. In Proceedings of the 2016 International Symposium on Power Line Communications and Its Applications (ISPLC), Bottrop, Germany, 20–23 March 2016; pp. 150–155.
45. Cavdar, I.; Engin, K. Measurements of Impedance and Attenuation at CENELEC Bands for Power Line Communications Systems. *Sensors* **2008**, *8*, 8027–8036. https://doi.org/10.3390/s8128027.
46. Avram, S. Power Line Communication Channel Noise Source Detection Using Smart Meters. In Proceedings of the 2016 12th IEEE International Symposium on Electronics and Telecommunications (ISETC), Timisoara, Romania, 27–28 October 2016; p. 106.
47. Szymczyk, C.; Nieß, N.; Breitenbach, J.N.; Bumiller, G. Calibration Method for an On-Line PLC Blocking Filter Characterization System. In Proceedings of the 2023 IEEE International Symposium on Power Line Communications and Its Applications (ISPLC), Manchester, UK, 21–22 March 2023; pp. 25–30.
48. Nieß, N.; Breitenbach, J.N.; Szymczyk, C.; Bumiller, G. Comprehensive Approach to on Line EMI Filter Characterization at Full Load Current. In Proceedings of the 2023 IEEE International Symposium on Power Line Communications and Its Applications (ISPLC), Manchester, UK, 21–22 March 2023; pp. 31–36.
49. *EN 50065-7*; Signalling on Low-Voltage Electrical Installations in the Frequency Range 3 KHz to 148.5 KHz—Part 7: Equipment Impedance. Available online: https://knowledge.bsigroup.com/products/signalling-on-low-voltage-electrical-installations-in-the-frequency-range-3-khz-to-148-5-khz-equipment-impedance/standard (accessed on 29 April 2023).
50. Randus, M.; Hoffmann, K. A Simple Method for Extreme Impedances Measurement—Experimental Testing. In Proceedings of the 2008 72nd ARFTG Microwave Measurement Symposium, Portland, ON, USA, 9–12 December December 2008; pp. 40–44.
51. Keysight Technologies Ultra-Low Impedance Measurements Using 2-Port Measurements. Available online: Literature.Cdn.Keysight.Com/Litweb/Pdf/5989-5935EN.Pdf (accessed on 14 April 2023).
52. Novak, I. Why S11 VNA Measurements Don't Work for PDN Measurements. Available online: http://www.electrical-integrity.com/Quietpower_files/QuietPower-4.pdf (accessed on 4 April 2023).
53. *EN 50470-1:2006+A1:2018*; Electricity Metering Equipment (a.c.). General Requirements, Tests and Test Conditions. Metering Equipment (Class Indexes A, B and C). Available online: https://knowledge.bsigroup.com/products/electricity-metering-equipment-a-c-general-requirements-tests-and-test-conditions-metering-equipment-class-indexes-a-b-and-c/standard (accessed on 29 April 2023).
54. *EN 61000-4-5:2014+A1:2017*; Electromagnetic Compatibility (EMC)—Part 4–5: Testing and Measurement Techniques. Surge Immunity Test. 2014. Available online: https://knowledge.bsigroup.com/products/electromagnetic-compatibility-emc-testing-and-measurement-techniques-surge-immunity-test-2/standard (accesed on 29 April 2023).
55. *EN 50470-3:2006+A1:2018*; Electricity Metering Equipment (a.c.). Particular Requirements. Static Meters for Active Energy (Class Indexes A, B and C). Available online: https://knowledge.bsigroup.com/products/electricity-metering-equipment-a-c-particular-requirements-static-meters-for-active-energy-class-indexes-a-b-and-c/standard (accessed on 29 April 2023)
56. *EN 50160:2010+A3:2019*; Voltage Characteristics of Electricity Supplied by Public Electricity Networks. Available online: https://knowledge.bsigroup.com/products/voltage-characteristics-of-electricity-supplied-by-public-electricity-networks/standard (accessed on 29 April 2023).
57. TMOV—Littelfuse. Available online: https://www.littelfuse.com/products/varistors/thermally-protected/tmov.aspx (accessed on 30 April 2023).
58. Varistors—An Overview. ScienceDirect Topics. Available Online: https://www.sciencedirect.com/topics/materials-science/varistors (accessed on 30 April 2023).
59. Wu, W.; Xie, Z.; Chen, Y.; Liu, J.; Guo, J.; Xu, Y.; Wang, H.; Luo, A. Analysis and Suppression of High-Frequency Oscillation between Converter-Based Source and Loads in an Island Power System. *Int. J. Electr. Power Energy Syst.* **2020**, *117*, 105616. https://doi.org/10.1016/j.ijepes.2019.105616.

60. Corporation, R.-M.O. Surge Safety Resistor—SSR. Made in Taiwan MELF Resistors Manufacturer—FIRSTOHM. Available online: https://www.firstohm.com.tw/en/category/CATE-surge_safety_resistor-SSR.html?page=13 (accessed on 30 April 2023).
61. Creepage Distance—An Overview. ScienceDirect Topics. Available online: https://www.sciencedirect.com/topics/engineering/creepage-distance (accessed on 30 April 2023).
62. JFG—Axial Metallized Polyester & Polypropylene Film Capacitor—Jb. Available online: https://www.jbcapacitors.com/Plastic-Film-Capacitors/JFG-Axial-Metallized-Polyester-Polypropylene-Film-Capacitor.html (accessed on 30 April 2023).
63. MS-184075-2-DataSheet.Pdf. Available Online: Https://Datasheets.Micrometals.Com/MS-184075-2-DataSheet.Pdf (accessed on 12 April 2023).
64. Inoue, A.; Kong, F. Soft Magnetic Materials. In *Encyclopedia of Smart Materials*; Olabi, A.-G., Ed.; Elsevier: Oxford, UK, 2022; pp. 10–23; ISBN 978-0-12-815733-6.
65. Touchstone Format—Touchstone Format—Keysight Knowledge Center. Available online: https://edadocs.software.keysight.com/display/genesys2010/Touchstone+Format (accessed on 30 April 2023).
66. Caspers, F. RF Engineering Basic Concepts: S-Parameters. Available Online: https://cds.cern.ch/record/1415639/files/p67.pdf (accessed on 20 April 2023).
67. Liu, S.; Zhang, Y.; Yu, D. Research and Design of EMI Digital Filters Using Scattering Parameters. In Proceedings of the 2009 International Conference on Wireless Communications Signal Processing, Nanjing, China, 13–15 November 2009; pp. 1–5.
68. Taking Advantage of S-Parameter. Available Online: Https://Product.Tdk.Com/En/Products/Emc/Guidebook/Eemc_basic_03.Pdf (accessed on 20 April 2023).
69. R&S®ZNB Vector Network Analyzer Specifications. Available Online: Https://Scdn.Rohde-Schwarz.Com/Ur/Pws/Dl_downloads/Dl_common_library/Dl_brochures_and_datasheets/Pdf_1/Service_support_30/ZNB_dat-Sw_en_5214-5384-22_v0900_96dp.Pdf (accessed on 2 April 2023).

Disclaimer/Publisher's Note: The statements, opinions and data contained in all publications are solely those of the individual author(s) and contributor(s) and not of MDPI and/or the editor(s). MDPI and/or the editor(s) disclaim responsibility for any injury to people or property resulting from any ideas, methods, instructions or products referred to in the content.